Electrochemical and electronic detection of biomarkers in serum: a systematic comparison using aptamer-functionalized surfaces

Vladyslav Mishyn, Teresa Rodrigues, Yann R. Leroux, Laura Butruille, Eloise Woitrain, David Montaigne, Patrik Aspermair, Henri Happy, Wolfgang Knoll, Rabah Boukherroub, et al.

Electrochemical and electronic detection of biomarkers in serum: A systematic comparison using aptamer-based receptors

Vladyslav Mishyn,[1]*" Teresa Rodrigues,[1,2]*" Yann R. Leroux,[3] Laura Butruille,[4] Eloise Woitrain,[4] David Montaigne,[4] Patrik Aspermair,[2] Henri Happy,[1] Wolfgang Knoll,[2,5] Rabah Boukherroub[1] and Sabine Szunerits[1*]

[1]*Univ. Lille, CNRS, Centrale Lille, Univ. Polytechnique Hauts-de-France, UMR 8520 - IEMN, F-59000 Lille, France*

[2]*Austrian Institute of Technology, Biosensor Technologies, Konrad-Lorenz-Strasse 24, 3430 Tulln, Austria*

[3]*Univ. Rennes, CNRS, ISCR –UMR 6226, Campus de Beaulieu, F-35000 Rennes, France*

[4]*Univ. Lille, Inserm, CHU Lille, Institut Pasteur de Lille, U1011-EGID, 59000 Lille, France*

[5]*Department of Physics and Chemistry of Materials, Faculty of Medicine/Dental Medicine, Danube Private University, Krems, Austria*

*Corresponding authors: vladyslav.mishyn@univ-lille.fr (VM); Teresa.Rodrigues@ait.ac.a (TR)

" equal contributions

ABSTRACT

Sensitive and selective detection of biomarkers in serum in a short time has a significant impact on health. The enormous clinical importance of developing reliable methods and devices for testing serum levels of cardiac troponin I (cTnI), which are directly correlated to acute myocardial infarction (AMI), has spurred an unmatched race among researchers for the development of highly sensitive and cost-effective sensing formats to be able to differentiate patients with early onset of cardiac injury from healthy individuals with a mean cTnI level of 26 pg mL−1. Electronic- and electrochemical-based detection schemes allow for fast and quantitative detection not otherwise possible at the point of care. Such approaches rely largely on voltammetric and field-effect-based readouts. Here, we systematically investigate electric and electrochemical point-of-care sensors for the detection of cTnI in serum samples by using the same surface receptors, cTnI aptamer-functionalized CVD graphene-coated interdigated gold electrodes. The analytical performances of both sensors are comparable with a limit of detection (LoD) of 5.7 ± 0.6 pg mL−1(electrochemical) and 3.3 ± 1.2 pg mL−1 (electric). However, both sensors exhibit different equilibrium dissociation constant (KD) values between the aptamer-linked surface receptor and the cTnI analyte, being 160 pg mL−1 for the electrochemical and about three times lower for the electrical approach with KD = 51.4 pg mL−1. This difference is believed to be related to the use of a redox mediator in the electrochemical sensor for readout. The ability of the redox mediator to diffuse from the

solution to the surface via the cTnI/aptamer interface is hindered, correlating to higher KD values. In contrast, the electric readout has the advantage of being label-free with a sensing limitation due to ionic strength effects, which can be limited using poly(ethylene) glycol surface ligands.

Keywords: aptamer, graphene-based field effect transistor, differential pulse voltammetry, cTnI.

Introduction

According to United States Food and Drug Administration (FDA), an ideal biomarker should be specific for a particular disease, safe and easy to measure, allowing fast diagnosis and accurate results about the health state of a person [1]. This definition applies well to the protein biomarker troponin I (cTnI) where an early detection in patients with a higher risk of acute myocardial infarction (AMI) can reduce the risk of death from heart attack [2]. Several ways of cTnI diagnostics have been formulated since cTnI has become the gold standard for AMI diagnostics due to the correlation between AMI and cTnI level in blood [3, 4]. In particular, cTnI detection systems that are portable, use small sample volumes, and combine high sensitivity with short detection times are sought after lately [5–7]. While the first-generation assays were only able to detect high plasma concentrations (500 pg mL−1) of troponin [8], the next generation assays could identify heart injury earlier, but were not sensitive enough to recognize people at risk for MI. Finally, the last-generation highly sensitive troponin assays can differentiate patients with myocardial ischemia onset and can reliably detect the low troponin levels in healthy individuals, which correspond to a concentration of 26 pg mL−1 (1.05 pM) [9]. This is about 100–1000 times lower than the cTnI level in patients with a clear positive test for AMI, with serum levels of cTnI in the 5–50 ng mL−1 concentration range.

The fast response time of electric and electrochemical sensors makes them well-adapted for detecting cTnI in emergency settings. The current possibility of smartphone-based readouts and minimal sample volumes are some important features for point-of-care diagnostics if the required sensitivity can be reached. Lee et al. proposed recently an Au microgap chip modified with an Au nanospikes and a DNA three-wayjunction probe, comprising a cTnI recognition part, methylene blue for signal transduction, and a thiol group for surface immobilization. Using cyclic voltammetry, a limit of detection (LoD) for cTnI of 1 pM (24.8 pg mL−1) in human serum was achieved [10]. While a comparable LoD of 33 pg mL−1 was reported by the Dutra group using an electrochemical immunosensing concept [11], we proposed the use of nitrogen-doped reduced graphene oxide (N-prGO) as electrode material for cTnI quantification using differential pulse voltammetry (DPV) and [Fe(CN)6]4– redox probe for the readout. This sensor recorded a LoD of 0.88 pg mL−1 [12], perfectly adapted for distinguishing healthy patients from patients with myocardial ischemia onset. The question remains, is there still space for improvement through tailoring the surface architecture of the electrochemical sensors? In this paper, CVD graphene-coated interdigitated electrodes covalently modified with cTnI aptamers were used in an electrochemical and liquid-gated field-effect transistor formats alike for cTnI sensing. In terms of analytical performance, both approaches displayed comparable sensitivities, i.e. a LoD = 5.7 ± 0.6 pg mL−1 for electrochemical and 3.3 ± 1.2 pg mL−1 for electric readouts. The highly controlled surface chemistry allowed us to reach detection limits comparable to those of other cTnI sensors reported in the scientific literature, indicating that not much more improvement is expected to happen on 2D surface architectures under our experimental conditions without futher signal amplification. The difference in both detection schemes is the use of a redox mediator in the case of electrochemical sensing while the electric readout is a real label-free approach. Additionally, the use of poly(ethylene) glycol surface linkers overcomes partial limitations inherent for GFET in terms of ionic strength and sensing in serum.

Materials and Methods

Materials: Phosphate buffer tablets (P B S) , tetrabutylammonium fluoride (TBAF), copper(II) sulfate (CuSO4), L-ascorbic acid, ethylenediaminetetraacetic acid (EDTA), tetra-n-butylammonium hexafluorophosphate (NBu4PF6), methoxypolyethylene glycol azide PEG (average Mn = 1000), ammonium persulfate ((NH4)2S2O8), trimethoxyphenylsilane (TMPS), isopropyl alcohol (IPA), and ferrocenemethanol were purchased from Sigma-Aldrich and used as received. Azidomethylferrocene was synthesized according to reference [13]. 4-((Triisopropylsilyl) ethylenyl)benzenediazonium tetrafluoroborate (TIPS-Eth-ArN2+) was synthesized as reported previously [14]. The 5′-azide modified troponin I aptamer (5′-N3-TTT-TTT-CGTGCA GTA CGC CAA CCT TTC TCA TGC GCT GCC CCT CTT A-3′) was purchased from integrated DNA Technologies (Leuven, Belgium). A Human Cardiac Troponin I ELISA Kit (ref. ab200016) was purchased from ABCAM (Cambridge, UK). NP-32 peptide (MW = 3.4 kDa) was purchased from BACHEM AG (Switzerland). Interdigitated microelectrodes (ED-IDE1-Au w/o SU8) were provided by Micrux Technologies. The electrodes are made of gold (180 nm) with an adhesion layer of titanium (20 nm) deposited via physical-vapour deposition (PVD).

Surface modification: The synthesis of monolayer graphene and sensor fabrication as well as the strategy on electrografting of 4-((triisopropylsilyl)ethylenyl)benzenediazonium tetrafluoroborate (TIPS-Eth-ArN2+) were performed according to [15]. Ethynylmodified sensors were exposed to azide-terminated polyethylene glycol (mPEG-N3, Mn 1000) and azide-terminated aptamer mixtures (5 μM/10 μM) in a ratio of 1:2 using CuSO4 (0.01M) and Lascorbic acid as catalysts. The interface was then treated with an aqueous solution of EDTA (10 mM) for 10 min to chelate any remaining Cu2+ residues and finally washed copiously with water and dried at room temperature.

Electrochemical measurements: Electrochemical measurements were performed on a potentiostat/galvanostat/impedance analyser (PalmSens4, PalmSens, The Netherlands). A conventional three-electrode cell (Micrux, Spain) was employed using a silver wire covered with silver chloride (Ag/AgCl) and a platinum mesh as the reference and auxiliary electrodes, respectively. The IDEs were acting as a working electrode. The cyclic voltammograms during the electrochemical grafting were recorded with a scan rate of 50 mV s−1 and potential steps of 0.01 V. The differential pulse voltammograms for the sensing were obtained using

potential steps of 0.005 V, potential pulses of 0.06 V and a pulse time of 0.02 s and a scan rate of 100 mV s−1.

Electric sensing: Electric measurements were conducted using a probe station source meter unit U2322A (Keysight Technologies, USA) using a PMMA commercial flow cell (Micrux Technologies, Spain) with a flow rate of 50 µL min−1 [15]. A silver chloride wire was used to operate in a liquid-gate configuration.

Characterization: Scanning electron microscopy (SEM) images were recorded on an electron microscope ULTRA 55 (Zeiss, France). Raman spectroscopy measurements were performed on a LabRam HR Micro-Raman system (Horiba Jobin Yvon, France).

Human serum samples: Human serum samples were provided by CHU Lille from the ongoing clinical POMI-AF study (principal investigator David Montaigne; Clinical trial #NCT03376165), approved by the local ethics committee. Patients were included after informed consent before undergoing cardiac surgery, and blood samples were obtained one day following surgery to monitor peri-operative cardiac injury. For each patient, 4 mL of venous blood was collected on EDTA tubes (BD vacutainer), centrifugated and immediately aliquoted in 500 µL for storage (− 80 °C). The magnitude of myocardial injury was assessed thanks to the Human Cardiac Troponin I ELISA Kit (ref. ab200016) from ABCAM.

Results and discussion

Formation of ethynyl-terminated graphene-based electrodes for “click”-reaction-based coupling of cTnI aptamers.

Graphene-modified interdigitated gold electrodes (Au/G) were produced by wet-transfer of CVD-grown graphene on Cu foils. Figure 1a depicts a SEM image of the graphene coated IDE electrodes showing that the gold electrodes as well as the interelectrode spacing are covered with graphene nanosheets. The Raman spectrum of the formed Au/G electrode (Fig. 1b) consists of peaks at 1350, 1580 and 2706 cm−1 attributed to D (defects in the graphene sheet), G (sp2 carbon) and 2D (secondary D band), respectively. The intensity ratio between 2D and G bands (2D/G) is 2.04, indicating that the transferred graphene monolayer has low impurities and is of high quality. The intensity ratio between the D and G peaks (D/G) is 0.35 in the graphene lattice after transfer, indicating a low disorder. XPS analysis of the C1s core level spectrum of IDE/G is dominated by the band at 284.7 eV ascribed to the Csp2.

Additional bands at 285.0, 286.4 and 288.6 eV are due respectively to C-sp3 components, mostly present at the grain boundaries of the large graphene sheets, and edge functions such as C–O andC=O (Fig. 1c). These interfaces were used in the following for electrochemical surface functionalization, electrochemical (Fig. 1d) and electric cTnI sensing (Fig. 1e).

To realize biodetection of cTnI, a troponin-specific aptamer was covalently grafted onto the IDE/G chips, as outlined in Fig. 2a. First, IDE/G was modified with 4-[(triisopropylsilyl) ethylenyl]benzenediazonium tetrafluoroborate (TIPS-Eth-ArN2+) salt via electrochemical reduction as lately reported by us [15]. The reduction band of TIPS-Eth-ArN2+ located at around − 0.2 V vs. Ag/AgCl was strongly decreased already after the first reductive scan (Fig. 2b). The grafting process using the diazonium salt is self-terminated and completed after one cycle. The success of the electrografting was in addition validated by differential pulse voltammogram (DPV) using ferrocenemethanol as redox mediator (Fig. 2c), where a strong decline in the charge transfer current was observed in line with the grafting of the bulky triisopropylsilyl (TIPS) group on the electrode surface. Chemical deprotection of the TIPS groups resulted in the partial recovery of the ferrocenemethanol oxidation current in the DPV sensogram.

The transfer characteristics of the GFET (Fig. 2d) as a function of the gate voltage (VG) before and after electrografting of TIPS-Eth-ArN2+ revealed that electrochemical modification resulted in a positive shift of the Dirac point compared to the initial GFET, indicating a p-doping effect, with hole (μh) and electron (μe) mobilities reaching 1003 cm2 V−1 s−1 and 829 cm2 V−1 s−1, respectively. Chemical deprotection of the TIPS group with tetrabutylammonium fluoride (TBAF) did not alter the transfer characteristics of the GFET, but shifted the Dirac point back to more negative values. “Clicking” cTnI aptamer onto the ethynyl-terminated GFET induced another negative shift of the Dirac point without altering the charge mobilities being μh = 1200 cm2 V−1 s−1 and μe = 907 cm2V−1 s−1 which is important for a good sensing device.

To estimate the amount of aptamers immobilized via “click” chemistry to the Au/G electrodes and GFET devices, azidomethylferrocene (10 μM) was “clicked” to the surface as a model compound. From the CV in Fig. 2e, the surface coverage Γ can be estimated using Eq. (1):

$$\Gamma = Q/nFA \quad (1)$$

where Q is the passed charge (C), n the number of exchanged electrons (n = 1), F the Faraday constant (96.485 C mol−1) and A the electroactive surface of the electrode determined as 0.1

cm2. Clicking azidomethylferrocene (10 μM N3-ferrocene) to the ethynyl-terminated sensors resulted in a surface coverage of Γ = 5.9 × 10−11 mol cm−2. Considering ferrocene molecules as spheres with a diameter of 6.6 Å, with a maximum coverage being estimated at Γ = 4.4 × 10−10 mol cm2 [16], this corresponds to 13% of the maximum surface coverage. The amount of the linked receptor can be further controlled by diluting azidomethylferrocene with N3-terminated poly(ethylene glycol) (PEG). To ensure a sensor with good anti-fouling properties, a mixture of N3-modified ferrocene and N3-terminated poly(ethylene glycol) (PEG) in a mass ratio of 1:2 and 2:1 (aptamer/PEG) was in addition employed. Ferrocene coverages of Γ= 3.0 × 10−11 mol cm−2 (ferrocene:PEG = 2:1) and Γ = 1.02 × 10−11 mol cm−2 (ferrocene:PEG = 1:2) were determined, respectively, corresponding to 6 and 2% of the theoretical coverage, respectively. The use of the PEG chain is believed to be not only beneficial as anti-fouling, but also to have a positive effect on the Debye length screening limitation [17].

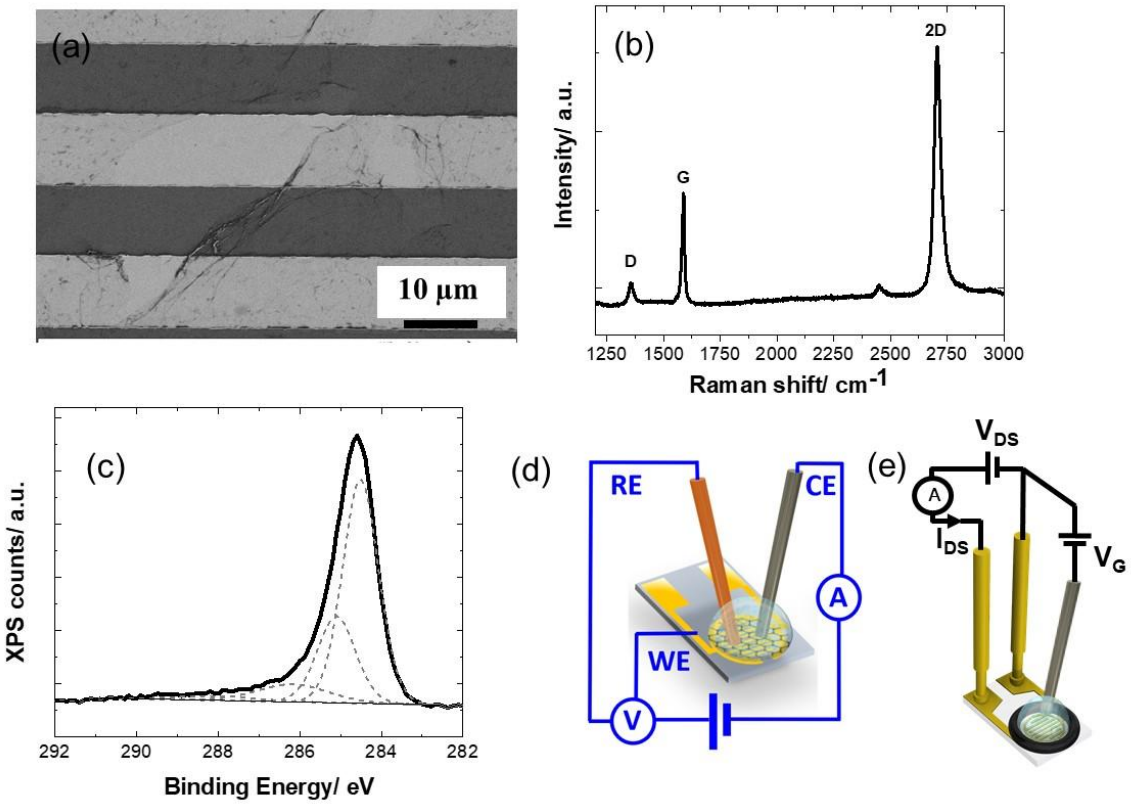

Figure 1. Characterization of graphene-based electrodes for electrochemical surface modification and sensing: (a) SEM image of the IDE chip after coating with CVD graphene showing full coverage over the gold lines as well as the space between IDE. (b) Raman spectrum of the graphene channel. (e) C1s core level spectrum of the electrode. (d) Scheme of

the electrochemical set up used for modification and cTnI electrochemical sensing. (e) Liquid-gate based electric sensing scheme.

Electrochemical performance of the as-prepared IDE/G chip for cTnI sensing

To understand if such a controlled surface architecture allows improved cTnI sensing, DPV using ferrocenemethanol as redox mediator was applied for sensing the cTnI-aptamer interactions. When cTnI binds to the aptamer-modified electrode, a reduction in current was observed (Fig. 3a), as previously reported on other aptamer-functionalized interfaces [12].

Using the Langmuir isotherm format (Fig. 3b) and assuming a 1:1 complex between cTnI from solution and the aptamer receptor on the surface, a dissociation constant KD = 160 pg mL−1 was determined. This value was much lower than the literature-reportedKD of 270 pM (6480 pg mL−1) [18]. The lower the bulk concentration to reach half saturation of the sensor, the better is the sensitivity. With an estimated noise level of 1 µA and a Δj/ΔCcTnI determined as 0.52 µA cm−2/pg mL−1, a detection limit, defined as LoD = (3 × noise)/sensitivity, of 5.7 ± 0.6 pg mL−1 was determined.

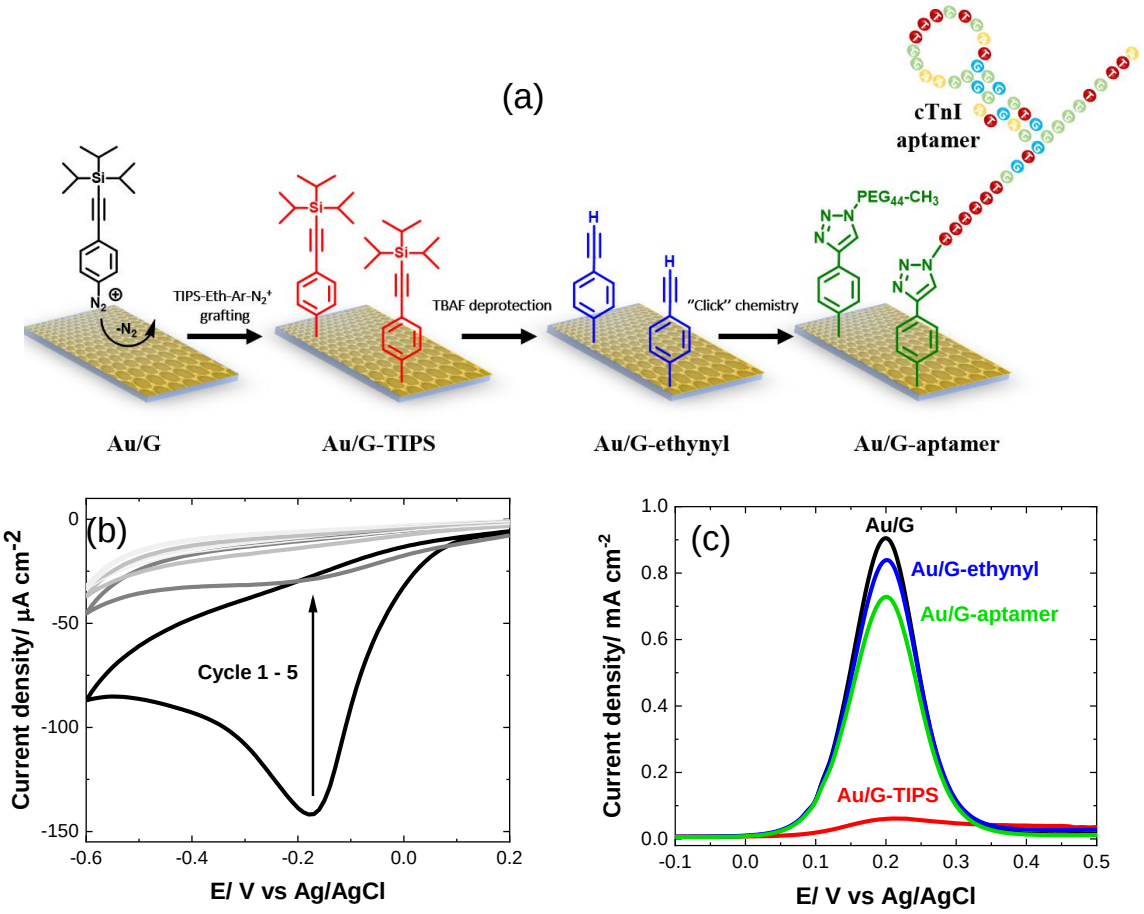

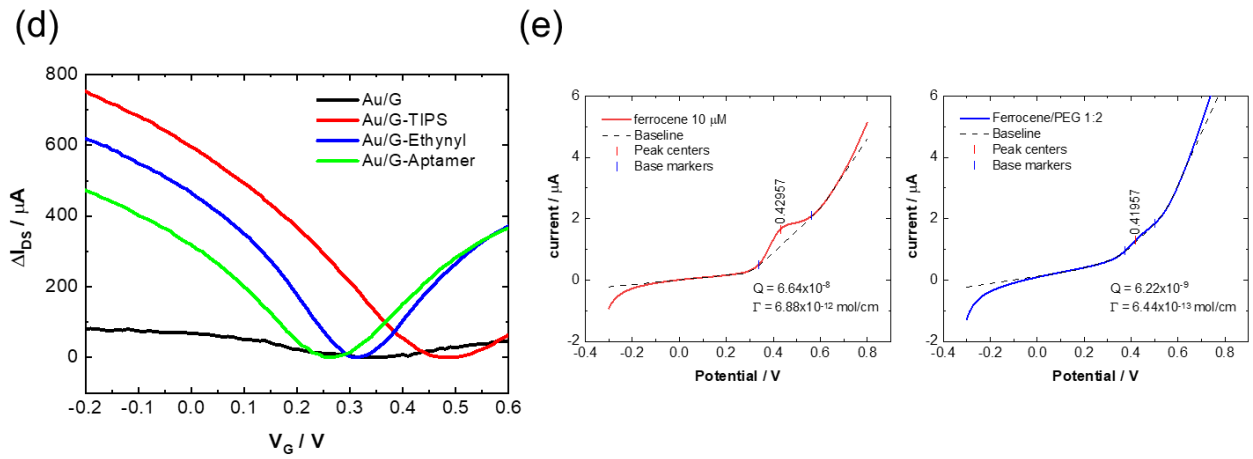

Figure 2. Formation of ethynyl-terminated graphene based electrodes: (a) Formation of ethynyl-terminated electordes (Au/G-ethynyl) via electrochemical reduction of TIPS-Eth-ArN_2^+ fomring Au/G-TIPS followed by TIPS deprotection using TBAF. Integration of surface receptors using Cu(I) catlysed click chemistry. (b) Electrochemical reduction of a solution of TIPS-Eth-ArN_2^+ (10 mM) in 0.1 M *n*-tetrabutylammonium hexafluorophosphate (nBu$_4$PF$_6$) in acetonitrile via cycling between +0.2 V and -0.6 V (vs. Ag/AgCl) at a scan rate of 50 mVs^{-1}. The reduction peak is visible at approximately -0.2 V vs. Ag/AgCl in the first scan and decreases in the subsequent scans. (c) Differential Pulse Voltammogram (DPV) of ferrocenemethanol (1 mM, 1xPBS) on Au/G (black), Au/G-TIPS (red), Au/G-ethynyl (blue) and Au/G-aptamer (green). (d) Electrical transfer characteristics of GFET (black), G-TIPS, G-ethynyl and and G-aptamer. (e) DPV of Au/G-ferrocene in ethanol/$LiClO_4$ (0.1 M), scan rate = 100 mVs^{-1}.

The binding affinity, quantified by the KD value, corresponds to the required analyte concentration to occupy 50% of the receptor aptamers on the electrode. This means that at the LoD, about 1.6% of the receptor ligands are occupied by the analyte. Compared to other electrochemical aptasensors, the sensor sensitivity is in line with the one reported using NprGO on GCE and more sensitive compared to others (Table 1). The good specificity of the sensor to cTnI was demonstrated using BNP-32 as analyte (Fig. 3d). The reproducibility of the electrode fabrication and its performance for cTnI sensing, expressed in terms of the relative standard deviation, was found to be 3.2% at a cTnI concentration of 80 pg mL−1. The long-term stability of the sensor showed a loss of 5.3% when tested using 80 pg mL−1 of cTnI, after the electrode was stored at 4 °C for 1 month. Furthermore, the stable covalent bonding of the receptor gives the sensor good stability and could be reused at least 10 times after dissociation of receptor/analyte binding in 0.1 M NaOH.

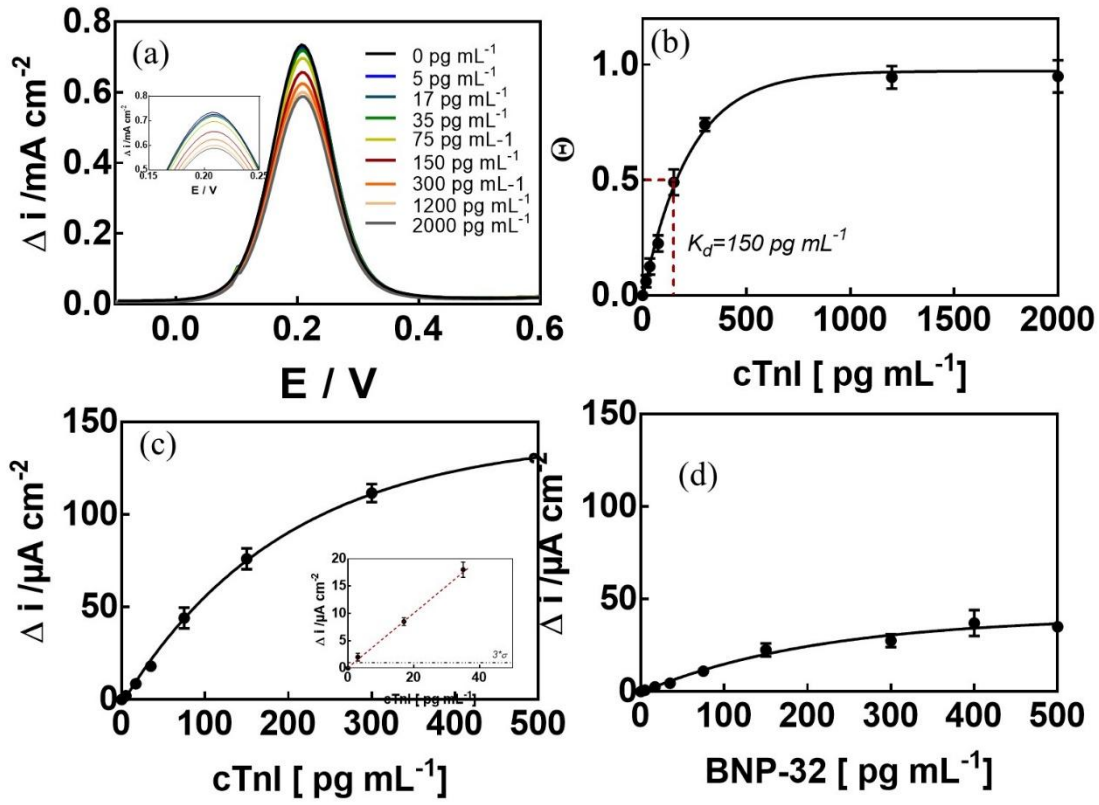

Figure 3. (A) Differential pulse voltammograms for different cTnI concentrations (0, 5, 17, 35, 75, 150, 300, 1200 and 2000 pg mL^{-1}) in 1 × PBS (pH 7.4) without washing steps. (b) Langmuir model of cTnI binding extracted form Figue 3a as a function of the analyte concentration of the solution running through the flow cell. (c) Calibration curve of CTnI in 1x PBS (pH 7.4). (d) Calibration curve of BNP-32 1 × PBS (pH 7.4) on CTnI apatamer modifed electrode.

Table 1: Compilation of Electrochemical aptasensors performances for the detection of cTnI.

Electrode architecture	**Method**	**Ligand attachement**	**LOD [pg mL^{-1}]**	**Linear range [ng mL^{-1}]**	**Ref.**
Au/ P1-P2-TdT/ apta	DPV	thiol	40	0.5–100	[17]
SPCE/ AuNPs/ TTCA/ apta	CA	NHS/EDC coupling	24	0.024–2.4	[18]
GCE/ MoS_2-apta	EIS	physisorption	22.8	0.24-24000	[19]
SPGE/MCH/DNA-NTH-apta/MMOF	DPV	thiol	16	0.05–100	[20]
Au/Au-ND/apta	DPV	thiol	8	0.05–500	[21]
IDE/G-apta	**DPV**	**click**	**5.7±0.8**	**0.0057-0.150**	**This work**
GCE/ N-prGO/ apta	DPV	π-π stacking	1	0.001-100	[15]

SPGE/ rGO-PEI-apta	DPV	π-π stacking	1	0.001-10	[22]

Apta: aptamer; CA: chronoamperometry; SPCE: screen-printed carbon electrode; SPGE: screen- printed gold electrode; TTCA: 5,2′:5′2″-terthiophene-3′-carboxylic acid; GCE: glassy carbon electrode; N-prGO: nitrogen-doped reduced graphene oxide; MCH: 6-Mercapto-1-hexanol; Au-ND: gold nanodumbbells; DNA-NTH: deoxyribonucleic acid nanotetrahedron; MMOF: magnetic metal organic framework; P1: 30-T CAT GCG GTT GGA AAG AG; P2: 50-CGC CAA CCT TTC TC-TTT-$(CH_2)_6$-SH; TdT: terminal deoxynucleotidyl transferase; MB-poly A: Methylene blue-AAA AAA AAA AAA; rGO: reduced graphene oxide; PEI: polyethylenimine; IDE: interdigitated electrodes.

Liquid-gated field-effect transistor performances of the as-prepared chip for cTnI sensing

The aptamer-modified interfaces were further employed asGFETs (Fig. 1d) and assessed for their ability to convert the binding with cTnI into an electric signal. The transfer characteristics in 0.01× PBS recorded after 10 min stabilization for each concentration of cTnI are presented in Fig. 4a. No change in the shape of the IDS/ VGS curves was observed besides a cathodic shift in theDirac point and a positive shift of the IDS in the electron regime. With an estimated noise level of 1.22 μA and a ΔIDS/ΔCcTnI determined as 1.09 μA/pg mL−1, a limit of detection equal to 3.3 ± 1.1 pg mL−1 (S/N = 3) was recorded. A KD = 54.9 pg mL−1 was calculated. This value is about 2 times lower than that determined by electrochemical means (Fig. 3b). However, the values are in the same order of magnitude and comparable to other field effect transistors reported so far (Table 2). As observed before for the electrochemical sensor, the electric aptamer sensor featured good specificity for cTnI (Fig. 4b), allowing to differentiate another cardiac biomaker, BNP-32.

The reproducibility of the IDS/VGS curves was determined to be excellent with a change in Dirac point position as low as 1.38% and a hole mobility of 2.24%. The long-term stability of the sensor showed a comparable loss of 4% when tested using 80 pg mL−1 of cTnI after the electrode was stored at 4 °C for 1 month.

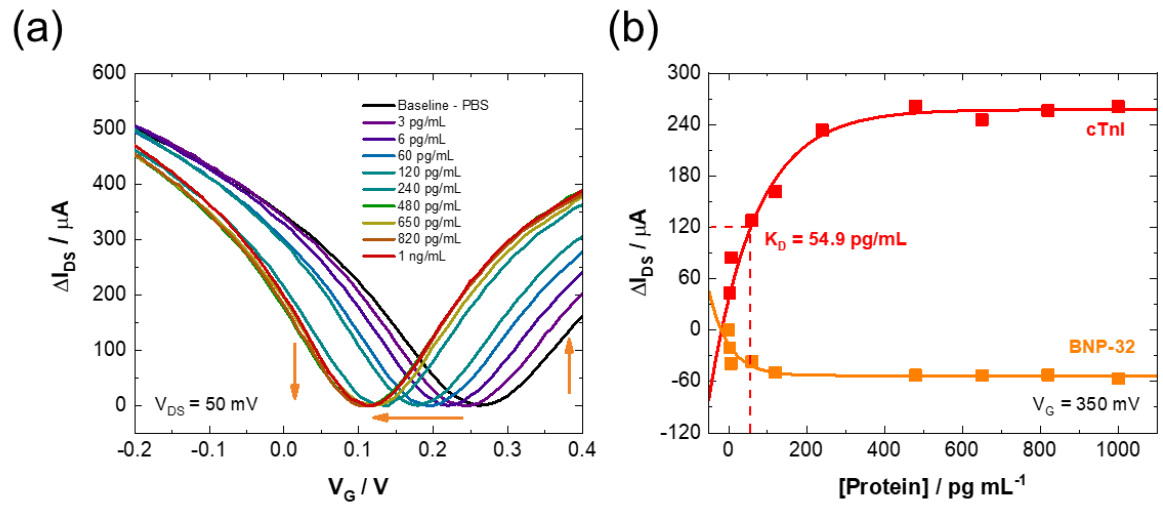

Figure 4: (a) Graphene transfer characteristics in 0.01× PBS (pH 7.4) without washing steps for different cTnI concentrations. Applied V_{DS} = 50 mV. (b) ΔI_{DS} for each cTnI concentration (red curve) and BNP-32 concentration (orange curve) at a fixed gate voltage V_G = 350 mV with respective Langmuir binding isotherm and estimated K_D.

Table 2: Compilation of Electrical aptasensors performances for the detection of cTnI.

Electrode architecture	**Method**	**Ligand attachement**	**LOD [pg mL^{-1}]**	**Linear range [ng mL^{-1}]**	**Ref**
CNN-GNPs/apta	ACEF	thiol	2400	2.4-2400	[23]
Si-NW/AzPTES/apta	FET	click	1000	1-1000	[24]
AlGaN/GaN/Au/apta	HEMT	thiol	6	0.006–148	[25]
G-aptamer	**GFET**	**click**	**3.3**	**0.003-0.15**	**This work**
AlGaN/GaN/Au/apta	HEMT	thiol	1	0.001-10	[26]

Si-NW: silicon nanowire ; AzPTES: (3-azidopropyl)triethoxysilane; HEMT: high-electron-mobility transistor; ACEF: alternating current electrothermal flow; CNN: carbon nanotube network; GNPs: gold nanoparticles; STV: streptavidin; DC: direct current

Clinical Relevance of both sensors.

Both sensors are within the clinical important window, i.e. 25 to 500 pg mL−1, allowing for differentiation between healthy people and those with low and high risk for myocardial infraction (AMI). In the case of the electric sensor, the device's response is, however, highly dependent on the ionic strength of the solution due to Debye screening effects (Fig. 5a). Indeed shifting from 0.01× PBS to 1× PBS (corresponds to serum) had a strong effect on the detected ΔIDS for each cTnI concentration. In contrast, electrochemical sensing in serum spiked with cTnI correlates well with the results of sensing in 1× PBS (Fig. 5b). Concerning the electrochemical sensor, the analytical sensitivity remained comparable even when performed in serum, with a noise level of 1.5 µA, a Δj/ΔCcTnI determined as

0.58 µA cm−2/pg mL−1, resulting in a LoD = 7.8 ± 2.3 pg mL−1. This contrasts to the GFET-based aptamer sensor, where the sensitivity is medium-dependent. The LoD value increased from4 to 39 pgmL−1 upon enhancing the ionic strength from 0.01× PBS to 0.1× PBS and reached 49 pg mL−1 in 1× PBS, equal to serum, respectively. Indeed, as pointed out by Nakatuka et al., surface confined PEG units allow ionic strengh buffering, making FET devices useful in higher ionic strengh media [29]. With a 20-times-higher LoD in serum, the GFETbased aptamer sensor should still be able to discriminate patients with moderate AMI symptoms with a cTnI level higher than 15 pg mL−1, but lower than 500 pg mL−1.

Samples of 6 patients with different troponin levels were analysed by both diagnostic devices. Using an ELISA cTnI assay, these samples were categorized into three zones: patients with mild (cTnI < 15 pg mL−1), moderate (15 pg mL−1 > cTnI < 500 mL−1) and severe (cTnT > 500 pg mL−1) AMI symptoms. Both sensors (Fig. 5c) are in agreement with ELISA results for cTnI concentrations lower than 500 pg mL−1 (electrochemical sensor) and 800 pg mL−1 (electric sensor), which correspond to the saturation of each sensor.

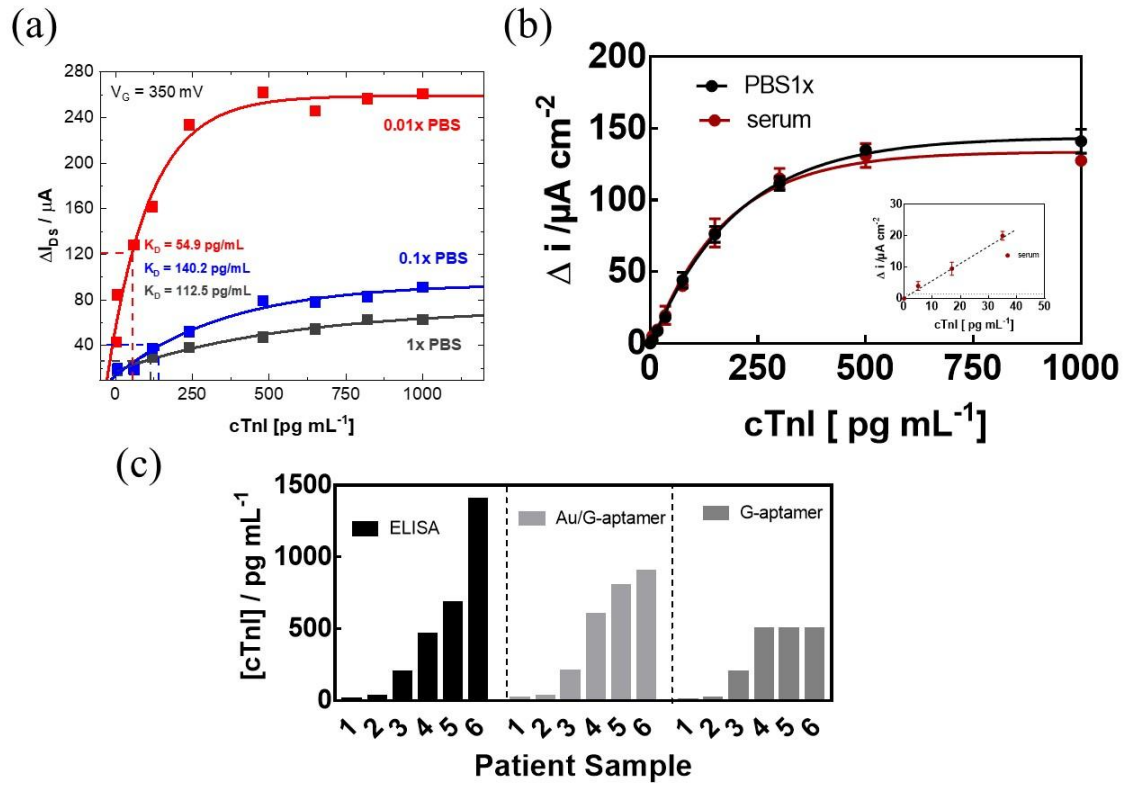

Figure 5: (a) Graphene transfer characteristics for cTnI concentration in 0.001× PBS (pH 7.4) (black) and 0.1× PBS (pH 7.4) (blue) applied V_{DS} = 50 mV. (b) Change in DPV current for different cTnI concentraitons in 1 × PBS (pH 7.4) (green) and in spiked serum smaples. (c) Analysis of 6 patient samples via ELISA and both diagnostic sensors: 3 groups of patients: low levels of troponin via ELISA (cTnI <15 pg mL^{-1}), moderate (15 pg mL^{-1}> c-TnI <500 mL^{-1}), and severe (cTnT >500 pg/mL) AMI synthoms.

Conclusion

In summary, we have developed a graphene-based aptamer sensor and evaluated its electrochemical and electric profiles for cTnI sensing in serum samples. Both sensors were based on gold IDE coated with graphene and modified via an electrografting process resulting in ethynyl-terminated electrodes to which the cTnI aptamer was covalently grafted using "click" chemistry. The majority of graphene-based sensors are based on non-covalent pyrene-based approaches, which generally results in low long-time stability and reproducibility. The covalent grafting strategy outlined here produces a highly stable and reproducible biosensor strategy and was successfully applied for electrochemical and electrical sensing of cTnI. Both architectures allowed for cTnI sensing below the clinically relevant 15 pg mL−1 cutoff level and enabled to determine the onset of moderate AMI. In the case of the electrochemical sensor, the readout necessitates a redox mediator, while a label-free approach could be employed for a GFET based aptamer sensor by simply following the change of ΔIDS for each cTnI concentration. The advantage of GFET-based sensing of cTnI is related to the low LoD and the low affinity constant determined, lower than the majority of aptamer/cTnI values. The electrochemical read shows about 3 times higher KD. The difference in the determined KD values on both sensors is believed to be related to the used protocol of sensing, as in the electrochemical sensor a redox mediator is employed. The drawback with the electrochemical sensor is based on the ability of the redox mediator to diffuse from the solution to the surface via the cTnI/aptamer interface. The observed diminution of the signal is directly correlated to the increase in steric hindrance of the cTnI/aptamer interface when increasing cTnI concentration. While using the GFET-based aptamer sensor, the change of the potential (cTnI/aptamer) interface is the guiding rule for the sensitivity of the sensor.

Acknowledgements

Financial support from the Centre National de la Recherche Scientifique (CNRS), the University of Lille, the Hauts-de- France region and the CPER "Photonics for Society" is gratefully acknowledged. Financial support came further from the FFG, Austria, within the Comet program.

Conflicts of Interest: "The authors declare no conflict of interest."
S. Szunerits is editor of Analytical and Bioanalytical Chemistry but was not involved in the peer review of this paper.

References

1. Sahu P, Pinkalwar N, Dubey RD, Paroha S, Chatterjee S, Chatterjee T. Biomarkers: an emerging tool for diagnosis of a disease and drug development. Asian J Pharm Sci. 2011;1:9–16.
2. Sinitskii A, Dimiev A, Corley DA, Fursina AA, Kosynkin DV, Tour JM. Kinetics of diazonium functionalization of chemically converted graphene nanoribbons. ACS Nano. 2010;4:1949–54.
3. Jaffe AS, Babuin L, Apple FS. Biomarkers in acute cardiac disease: the present and the future. J Am Coll Cardiol. 2006;48:1–11. 4. Masson J-F, Battaglia TM, Khairallah P, Beaudoin S, Booksh KS. Quantitative measurement of cardiac markers in undiluted serum. Anal Chem. 2007;79:612–9.
5. Jiang DE, Sumpter BG, Dai S. How do aryl groups attach to a graphene sheet? J Phys Chem B. 2006;110:23628–32.
6. Altintas Z, Fakanya WM, Tothill IE. Cardiovascular disease detection using bio-sensing techniques. Talanta. 2014;128:177–86.
7. Sarangadharan I, Wang S-L, Sukesan R, Chen P-C, Dai T-Y, Pulikkathodi AK, Hsu C-P, Chiang H-HK, Liu LY-M, WangY-L. Single drop whole blood diagnostics: portable biomedical sensor for cardiac troponin I detection. Anal Chem. 2018;90:2867–74.
8. Hamm CW, Goldmann BU, Heeschen C, Kreymann G, Berger J, Meinertz T. Emergency room triage of patients with acute chest pain by means of rapid testing for cardiac troponin T or troponin I. New Engl J Med. 1997;337:1648–53.
9. UpashamS, Tanak A, Prasad S. Cardiac troponin biosensors: where are we now. Adv Heal Care Technol. 2018;4:1–13.
10. Lee T, Lee Y, Park SY, Hong K, Kim Y, Park C, Chung Y-H, Lee M-H, Min J. Fabrication of electrochemical biosensor composed of multi-functional DNA structure/au nanospike on micro-gap/PCB system for detecting troponin I in human serum. Colloids Surf B. 2019;175:343–50.
11. Gomes-Filho S, Dias A, Silva M, Silva B, Dutra R. A carbon nanotube-based electrochemical immunosensor for cardiac troponin T. Microchem. 2013;109:10–5.
12. Chekin F, Vasilescu A, Jijie R, Singh SK, Kurungot S, Iancu M, Badea G, Boukherroub R, Szunerits S. Sensitive electrochemical detection of cardiac troponin I in serum and saliva by nitrogendoped porous reduced graphene oxide electrode, Sens. Actuators, B., 187. 2018;262:180.
13. Casas-Solvas JM, Vargas-Berenguel A, Capitán-Vallvey LF, Santoyo-González F. Convenient methods for the synthesis of ferrocene−carbohydrate conjugates. Org Lett. 2004;6:3687–90.

14. Leroux YR, Hapiot P. Nanostructured monolayers on carbon substrates prepared by electrografting of protected aryldiazonium salts. Chem Mater. 2013;25:489–95.
15. Mishyn V, Rodrigues T, Leroux Y, Aspermair P, Happy H, Bintinger J, Kleber C, Boukherroub R, Knoll W, Szunerits S. Controlled covalent functionalization of graphene-channel of a field effect transistor as ideal platform for (bio) sensing applications . Nanoscale Horiz. https: //doi.org/10.1039/D1NH00355K(2021).
16. Chidsey CE, Bertozzi CR, Putvinski T, Mujsce A. Coadsorption of ferrocene-terminated and unsubstituted alkanethiols on gold: electroactive self-assembled monolayers. J Am Chem Soc. 1990;112:4301–6.
17. Gao N, Gao T, Yang X, Dai X, Zhou W, Zhang A, Lieber CM. Specific detection of biomolecules in physiological solutions using graphene transistor biosensors. Proc Natl Acad Sci USA. 2016;113:14633–8.
18. Jo H, Gu H, JeonW, Youn H, Her J, Kim S-K, Lee J, Shin JH, Ban C. Electrochemical aptasensor of cardiac troponin I for the early diagnosis of acute myocardial infarction. Anal Chem. 2015;87: 9869–75.
19. LangM, Luo D, Yang G,Mei Q, Feng G, Yang Y, Liu Z, Chen Q, Wu L. An ultrasensitive electrochemical sensing platform for the detection of cTnI based on aptamer recognition and signal amplification assisted by TdT. RSC Adv. 2020;10:36396–403.
20. Jo H, Her J, Lee H, Shim Y-B, Ban C. Highly sensitive amperometric detection of cardiac troponin I using sandwich aptamers and screen-printed carbon electrodes. Talanta. 2017;165:442–8.
21. Qiao X, Li K, Xu J, Cheng N, Sheng Q, Cao W, Yue T, Zheng J. Novel electrochemical sensing platform for ultrasensitive detection of cardiac troponin I based on aptamer-MoS2 nanoconjugates. Biosens Bioelectron. 2018;113:142–7.
22. Sun D, LuoZ LJ, Zhang S, Che T, Chen Z, Zhang L. Electrochemical dual-aptamer-based biosensor for nonenzymatic detection of cardiac troponin I by nanohybrid electrocatalysts labelling combined with DNA nanotetrahedron structure. Biosens Bioelectron. 2019;134:49–56.
23. Negahdary M, Behjati-Ardakani M, Sattarahmady N, Yadegari H, Heli H. Electrochemical aptasensing of human cardiac troponin I based on an array of gold nanodumbbells-applied to early detection of myocardial infarction, Sens. Actuators, B. 2017;252:62–71.
24. Grabowska I, Sharma N, Vasilescu A, Iancu M, Badea G, Boukherroub R, Ogale S, Szunerits S. Electrochemical aptamerbased biosensors for the detection of cardiac biomarkers. ACS omega. 2018;3:12010–8.
25. Lee WC, Lee H, Lim J, Park YJ. An effective electrical sensing scheme using AC electrothermal flow on a biosensor platform based on a carbon nanotube network. Appl Phys Lett. 2016;109: 223701.
26. Kutovyi Y, Li J, Zadorozhnyi I, Hlukhova H, Boichuk N, Yehorov D, Menger M, Vitusevich S. Highly sensitive and fast detection of C-reactive protein and troponin biomarkers using liquid-gated single silicon nanowire biosensors. MRS Adv. 2020;5:835–46.
27. Sarangadharan I, Regmi A, Chen Y-W, Hsu C-P, Chen P-C, Chang W-H, Lee G-Y, Chyi J-I, Shiesh S-C, Lee G-B. High sensitivity cardiac troponin I detection in physiological environment using AlGaN/GaN high Electron mobility transistor (HEMT) biosensors.
Biosens Bioelectron. 2018;100:282–9.
28. Sinha A, Tai T-Y, Li K-H, Gopinathan P, Chung Y-D, Sarangadharan I, Ma H-P, Huang P-C, Shiesh S-C, Wang Y-L. An integrated microfluidic system with field-effect-transistor sensor
arrays for detecting multiple cardiovascular biomarkers from clinical samples. Biosens Bioelectron. 2019;129:155–63.

29. Nakatsuka N, YangK-A, Abendroth JM, CheungKM, Xu X, Yang H, Zhao C, Zhu B, Rim YS, Yang Y. Aptamer–field-effect transistors overcome Debye length limitations for small-molecule sensing. Science. 2018;362:319–24.